Hindawi
International Transactions on Electrical Energy Systems
Volume 2023, Article ID 8685976, 15 pages
https://doi.org/10.1155/2023/8685976

Research Article

Atom Search Optimization-Based PV Array Reconfiguration Technique under Partial Shading Condition

Dahu Li,[1] Hongyu Zhou ,[2] Yue Zhou,[1] Yuze Rao,[1] and Wei Yao[2]

[1]*State Grid Hubei Electric Power Co. Ltd., Wuhan 430077, China*
[2]*State Key Laboratory of Advanced Electromagnetic Engineering and Technology (Huazhong University of Science and Technology), Wuhan 430074, China*

Correspondence should be addressed to Hongyu Zhou; hongyu_zhou@hust.edu.cn

Received 25 October 2022; Revised 17 November 2022; Accepted 23 March 2023; Published 17 April 2023

Academic Editor: Xueqian Fu

Photovoltaic (PV) reconfiguration is an effective solution for reducing the hot spot effect caused by partial shadows on PV arrays. This paper proposed an efficient atom search optimization- (ASO-) based PV reconfiguration method. The analysis and comparison with the other four reconfiguration methods were performed by three evaluation criteria, which are mismatch loss, fill factor, and standard deviation, respectively. The conclusion can be drawn that the efficiency, rapidity, and reliability of ASO are superior to those of other methods. Besides, a moving cloud shadow mode of 9×9-scaled PV array is designed in this paper, which can be widely recommended to thoroughly study a PV reconfiguration approach.

1. Introduction

With the continuous expansion of the scale of power construction, the problem of excessive energy consumption has reached an unprecedented level [1, 2]. As a nonrenewable resource, although fossil fuel has the advantages of strong flammability and high calorific values, its reserves are quite limited [3, 4]. The resulting deterioration of the ecological environment and global warming has brought a very serious threat to people's survival and safety [5]. Due to the increasing demand for energy and the decreasing reserves of fossil energy [6], renewable energy sources are gaining more and more attention and are gradually replacing most fossil fuels [7], and one of the most promising energy sources is solar energy [8].

The solar cell is the core of the photovoltaic (PV) power generation system, and its conversion efficiency determines the practical application capability of the entire system [9, 10]. The application of PV power generation systems is complicated, and the single solar cell element cannot meet the conversion requirements of photovoltaic panels for power signal conversion [11]. Thus, it is necessary to connect multiple solar cell structures in series to form a solar cell array to ensure the smooth application of PV systems [12]. In the PV power generation system, the PV array can be understood as a combined connection form of solar cell elements [13]. Under the condition that the light intensity does not change, the more the number of solar cell elements connected in series, the more power the solar cell array has and the stronger the conversion ability [14].

PV arrays, as the most commonly used device to obtain solar energy, are widely used. PV cells are nonlinear devices at the core of PV power generation, and their output characteristics cause the PV array to work at a certain operating voltage to generate maximum output power [15]. However, some unavoidable destructive factors greatly reduce the efficiency of photovoltaic arrays. Partial shading condition (PSC) occlusion is one of them, which not only makes the output power curve appear multipeaks but also causes damage to a PV panel and may reduce its service life [16, 17]. In centralized PV systems, the series-parallel (SP) structure and total-cross-tied (TCT) structure are two commonly used structures in PV arrays [15]. The advantages of the SP structure are that the structure is relatively simple and that installation is convenient. In the TCT structure, modules are first connected in parallel to achieve the

required output voltage, and then, these strings are connected in series to ensure that the output voltage reaches the voltage range required under normal operating conditions [18]. TCT is more stable and has higher efficiency than SP in most cases; thus, it is used in this paper to achieve better reconfiguration performance.

In recent years, some researchers have put forward a new idea to reduce the hot spot effect caused by partial shadows on PV arrays, which is called PV reconfiguration [19]. Specifically, reconfiguration means that the PV array changes the position or connection method of the corresponding components according to the type of shadow so as to balance the irradiance of each row or column and improve the output power of the array [20]. PV reconfiguration does not require manual intervention, and the whole process automatically achieves preset goals, which is more flexible and easier to implement [21]. Some researchers have developed a static PV reconfiguration technique to change the physical structure of PV panels. In this technique, PV modules that are shaded will be replaced by unshaded modules according to some established rules so as to keep the output current in different rows consistent, such as in the Sudoku method [22], zig-zag method [23], skyscraper puzzle [24], and Lo Shu method [25].

However, complex PSC will cause worse accuracy, efficiency, and performance of PV reconfiguration. Therefore, using the dynamic reconfiguration to dynamically balance each row of the photovoltaic array can facilitate the tracking of the maximum power point and lay a foundation for further improving the efficiency of PV systems [26]. Existing dynamic reconfiguration usually uses heuristic algorithms to gain the best reconfiguration solution, thus achieving fast and accurate optimization [27]. The switch matrix changes the electrical connection between modules according to the optimal configuration of the algorithm output, thus realizing photovoltaic reconfiguration. Figure 1 shows a schematic diagram of a switch matrix consisting of a single-pole multiple-throw switch. Some researchers proposed different matrix switches for photovoltaic arrays of different scales, which can reconfigure the array quickly and flexibly and effectively improve the average output power and conversion efficiency of the array [28]. The immediate purpose of PV array reconfiguration is to evenly distribute uneven shadows across the whole array. The premise of reconfiguration is to obtain the key parameters and data of PV arrays. In the static reconfiguration technique, irradiance and temperature as well as voltage and current through PV cells are collected and then transmitted to the computational model of PV arrays. Afterward, the control unit deduces the optimal configuration following certain strategies and then shifts the modules using mechanical devices. Similar to the static reconfiguration technique, the first step of a dynamic reconfiguration technique is to acquire the data by using various sensors. Subsequently, these data are imported into the computational model of PV arrays that can simulate the operation characteristics of the array. Then, the central control unit deduces the optimal configuration with the help of the reconfiguration algorithm. After that, the optimal configuration is transmitted to the switch matrix. As the execution unit, the switch matrix alters the electrical connection among panels or modules according to the new configuration. Through such a set of actions, the target of mitigating the impact of PSC and improving the power output is realized. The general structure of the reconfiguration technique is exhibited in Figure 2.

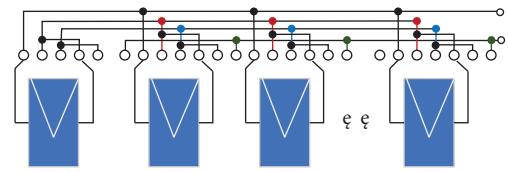

Figure 1: Structure of the switching matrix.

In [29, 30], detailed discussions of reconfiguration techniques that have been developed are given. In [31], the engineering practicability of the PV reconfiguration technique is illustrated. This paper proposed an atom search optimization-based PV reconfiguration method, which has better performance than other PV reconfiguration methods in this paper.

2. Modelling of PV Systems under the Shadow of Moving Clouds

2.1. Total-Cross-Tied PV System Modelling. A 9×9 TCT-interconnected PV array is used in this work, which is shown in Figure 3. TCT configuration is the most widely used connection and has been proved to be the most stable topology of PV arrays. It is worth noticing that this configuration technology does not change the original position of the PV array but changes its electrical connection. The total output voltage of the PV array can be written as follows:

$$V_{\text{out}} = \sum_{a=1}^{9} V_{\max a}, \tag{1}$$

$$\begin{aligned} I_{\text{out}} &= \sum_{a=1}^{9} \left(I_{ab} - I_{(a+1)b} \right) \\ &= 0, a, b \\ &= 1, 2, 3, \ldots, 9, \end{aligned} \tag{2}$$

where V_{out} is the output voltage of the PV array, I_{out} is the output current of the PV array, $V_{\max a}$ is the maximum voltage of ath row, and I_{ab} is the node current at the ath row and bth column.

In particular, Figure 4 shows the flowchart of PV reconfiguration based on ASO.

2.2. Shadow of Moving Cloud Modelling. In real projects, the shielding of large-scale PV arrays is mostly caused by clouds and the shape and position of clouds change continuously with time [32]. The output characteristics of the PV array are seriously affected by cloud covering situations. On this basis, the PV system needs to research and design the reconfiguration method, maximum power point tracking (MPPT), inverter, grid connection, and other measures to promote

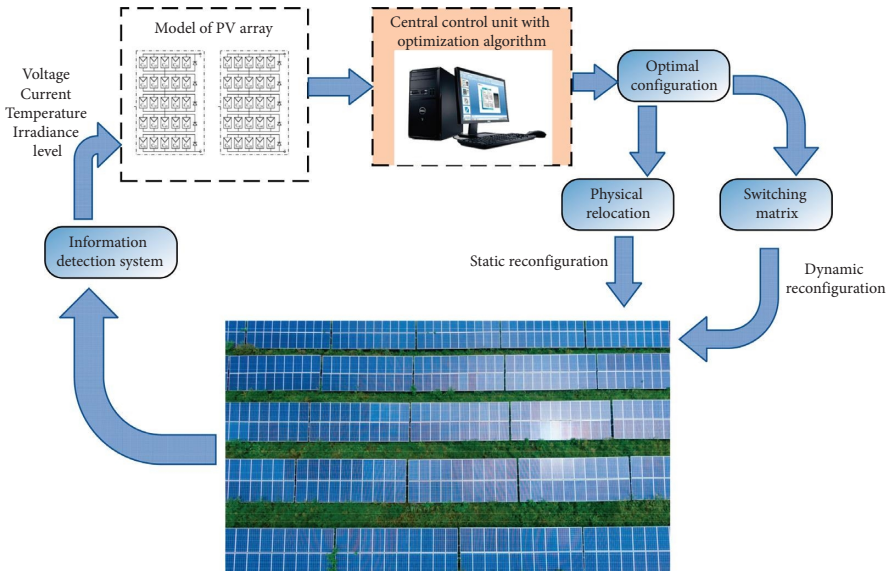

Figure 2: Structure of the reconfiguration technique.

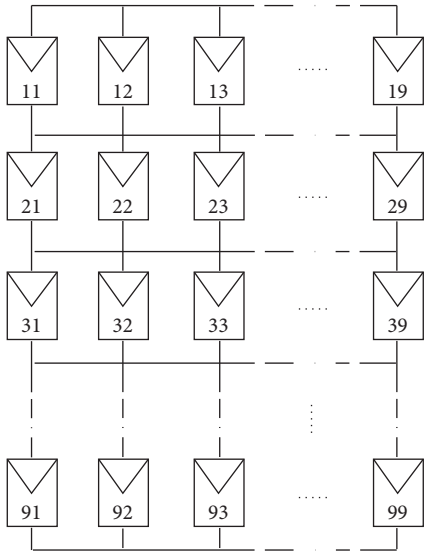

Figure 3: 9 × 9 TCT-connected array.

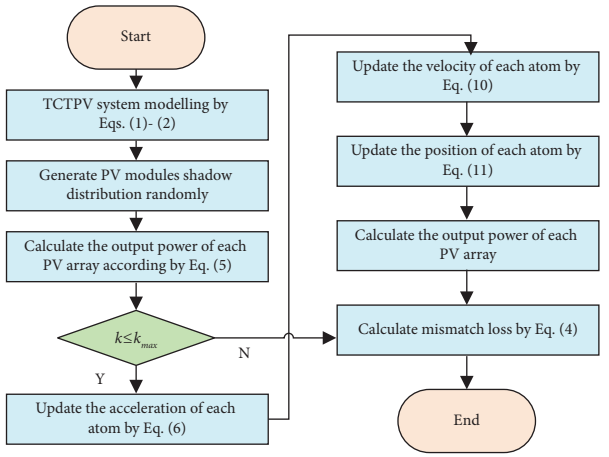

Figure 4: Flowchart of PV reconfiguration based on ASO.

the efficiency of the PV array. Therefore, it is necessary to establish the output characteristics model of the PV array in the case of moving cloud shading. By describing the moving cloud shadow itself and its motion factors, the target shadow of the object to be studied can be modelled [33]. Shadows blocking the PV array can be seen as projections on the horizontal plane of the PV array; hence, the movement of shadows can be regarded as the movement of particles.

This paper considered the shape of cloud and moving cloud shadows in 9 minutes with different irradiation values from 300 W/m^2 to 1000 W/m^2, which can offer reference for researchers in related fields.

2.3. Evaluation Criteria. There are three evaluation criteria to measure the simulation results of proposed ASO and other comparison methods. They are, respectively, (a) mismatch loss [20], (b) fill factor [20], and (c) standard deviation [34].

(i) Mismatch loss

The mismatch loss is defined as

$$P_{\mathrm{mi}} = P_{\mathrm{G(unshaded)}} - P_{\mathrm{G(shaded)}}, \tag{3}$$

where $P_{G(\mathrm{unshaded})}$ is the global maximum power of the unshaded PV system and $P_{\mathrm{G(shaded)}}$ is the global maximum power of the partially shaded PV system.

(ii) Fill factor

The fill factor (ff) is a critical criterion to denote the power loss of PV systems under PSC, which is given in the equation:

$$ff = \frac{V_{\mathrm{p}} \times I_{\mathrm{p}}}{V_{\mathrm{o}} \times I_{\mathrm{s}}}, \tag{4}$$

where V_p and I_p are the voltage and current of PV systems at the local maximum power point, respectively, and V_o and I_s are the open-circuit voltage and short-circuit current of the PV array, which are usually given by manufacturers.

(iii) Standard deviation

In this paper, standard deviation (STD) is used to evaluate the reconfiguration stability of heuristic algorithms.

2.4. Problem Formulation. When series-connected PV panels are all working properly under PS conditions, they will operate at points which are deviated from their maximum power point, respectively, resulting in a decrease in the obtained power. In order to impair the influence of mismatch loss caused by the occurrence of PSC, reconfiguration technologies are used to equalize the irradiation of each column and thus realize the maximization of output power, which can be written as

$$P_{\max} = \max\left(\sum_{a=1}^{9} I_a \bullet V_a\right), \tag{5}$$

where I_a and V_a represent the output current and output voltage of each row.

3. Atom Search Optimization-Based Reconfiguration Method

3.1. Mathematical Formulation of ASO. Atom search optimization is an efficient heuristic algorithm that was proposed by Zhao in 2019 [35]. It simulates the interatomic displacement caused by atomic attractive and repulsive forces in molecules. The mechanism of optimization is based on the specific mass and acceleration of different atoms, including update acceleration of atoms, update velocity of atoms and update position of atoms.

In the ASO algorithm, in order to strengthen the global exploration ability at the initial stage of iteration, each atom needs to interact with more neighboring atoms with better fitness. In the later stage of iteration, in order to enhance local development and promote algorithm convergence, each atom needs to interact with fewer neighboring atoms with better fitness.

It is assumed that an atom represents a PV module. The entire population consists of several atoms. It is worth noting that PV array reconfiguration changes the modules' electrical connection with different rows in the same column and hence balances the current of each line of modules. Atomic motion follows Newton's second law: the acceleration of the atom is related to its mass and is generated by the interaction between atoms and the geometric constraint of the optimal atom on it. Therefore, the acceleration of the ith atom at iteration t is as follows:

$$a_i(k) = \frac{F_i(k) + G_i(k)}{M_i(k)}, \tag{6}$$

where a_i is the acceleration of the ith PV module, $G_i(k)$ is the constraint force between atoms determined by positions and fixed bond length at kth iteration, $M_i(k)$ is the mass of the ith atom at kth iteration, and $F_i(k)$ is the total force acting on the ith atom at kth iteration, which can be expressed as follows:

$$\begin{aligned} G_i(k) &= -2\delta(k)\left(p_i(k) - p_{\text{best}}(k)\right), \\ F_i(k) &= \sum_{j \in N_{\text{best}}} r\left\{n(k)\left[h_{ij}^7(k) - 2h_{ij}^3(k)\right]\right\}, \\ M_i(k) &= \frac{e^{\left(f_i(k) - f_{\text{best}}(k)/f_{\text{best}}(k) - f_{\text{worst}}(k)\right)}}{\sum\left(f_i(k) - f_{\text{best}}(k)/f_{\text{best}}(k) - f_{\text{worst}}(k)\right)}, \end{aligned} \tag{7}$$

where $\delta(k)$ is the Lagrangian multiplier, which changes with the number of iterations, expressed by $\delta(k) = \beta e^{-20k/k_{\max}}$, β is the multiplier weight, p_i and p_{best} are the position of the ith atom and the best position among all atoms, respectively, r is a random number between [0, 1], $n(k)$ determines whether an atom is attracted or repulsed, which can be expressed by $n(k) = \alpha(1 - k - 1/k_{\max})^3 e^{-20k/k_{\max}}$, α is a weight factor, h_{ij} is the distance between two atoms, and $f_i(k)$, $f_{\text{best}}(k)$, and $f_{\text{worst}}(k)$ are the ith fitness value, best fitness value, and worst fitness value at kth iteration, respectively.

The velocity of the ith atom at kth iteration will be updated by the following equation:

$$v_i(k+1) = r_i v_i(k) + a_i(k). \tag{8}$$

The position of the ith atom at kth iteration will be updated by the following equation:

$$p_i(k+1) = p_i(k) + v_i(k+1). \tag{9}$$

3.2. Overall Process of ASO-Based PV Reconfiguration. The algorithm pseudocode of ASO-based PV reconfiguration is as follows (Table 1).

4. Case Studies

4.1. Classical 9 × 9 PV Array. To verify the effectiveness of the reconfiguration algorithm, various sizes of PV arrays and different shading modes are often simulated. In this section, the most frequently used 9 × 9 PV array is used to verify the effect of ASO, and the shadow of moving cloud in 9 minutes has been carried out to cooperate with the simulation experiment in this paper. The simulation tool used is MATLAB 2020a. Besides, the PV model and its parameters are provided in Table 2, and several reconfiguration methods, e.g., Sudoku [22], ant colony optimization (ACO) [36], genetic algorithm (GA) [37], and particle swarm optimization (PSO) [38], are also constructed for performance comparison. Run times, iteration, and the population number of each algorithm are set to be 20, 100, and 10, respectively. α and β of ASO are set to be 50 and 0.2, respectively. Figure 5 shows the shading mode of moving clouds in 9 minutes before reconfiguration. Figure 6 shows the best reconfiguration results of ASO in 9 minutes under the shadow of moving

Table 1: The detailed pseudocode of the ASO-based PV reconfiguration method.

(1): TCT PV system modelling by equations (1) and (2)
(2): **Initialize**: algorithms parameters (population number, iteration number, etc.)
(3): Generate PV module shadow distribution randomly
(4): Calculate the output power of each PV array according to equation (5) and keep it as the current optimal output power and optimal shadow distribution
(5): **While** $k \leq k_{\max}$
(6): Update the acceleration of each atom by equation (6)
(7): Update the velocity of each atom by equation (8)
(8): Update the position of each atom by equation (9)
(9): Calculate the output power of each PV array again and update the optimal shadow distribution and optimal output power
(10): Set $k = k + 1$
(11): **End while**
(12): **Output**: best shadow distribution of PV arrays and the maximum output power
(13): Calculate mismatch loss, *ff* of the optimal solution, and *STD* of simulation results of ASO in 20 runs

Table 2: The concrete parameter of PV modules.

Parameters	Value
Module	American Solar Wholesale ASW-280M
Number of parallel strings	1
Number of series-connected modules per string	1
Number of cells per module (Ncell)	72
Maximum power per module (W)	280.1567
Open-circuit voltage per module (V)	43.99
Short-circuit current per module (A)	8.14
Voltage at the maximum power point per module (V)	37.01
Current at the maximum power point per module (A)	7.57

clouds. It can be seen that the shadow is spread evenly compared to before reconfiguration.

When the PV array is optimized by ASO, the inner connection of the PV array is changed according to the best optimization result gained by the algorithm. The maximum optimized output power and the minimum output power of each heuristic algorithm in 20 run times and the mismatch loss and the fill factor of each method are presented in Table 3. It is apparent that heuristic algorithms get the best optimistic effect and that Sudoku takes second place. Among all algorithms, $P_{\max}$ and $P_{\min}$ gained by ASO are both higher than those obtained by other algorithms, and the STD of ASO is smaller than that of other algorithms, which illustrates the high stability of ASO. It is obvious that the mismatch loss and ff of ASO behave better in performance among all algorithms. The optimal mismatch loss gained by ASO is 38.13%, 20.93%, 2.49%, 3.75%, and 0.51% lower than that of before optimization, Sudoku method, ACO, GA, and PSO, respectively, and optimal *ff* gained by ASO is 20.70%, 7.95%, 0.71%, 1.15%, and 0.13% higher than that of before optimization, Sudoku method, ACO, GA, and PSO, respectively.

Figure 7 shows the output *I-U* curves and *P-U* curves of before optimization, Sudoku method, GA, and ASO in 9 minutes. It is observed that, when there are more shadows, output characteristic curves get less smooth. The output *I-U* curves usually have a lot of inflection points, and the output *P-U* curves have a lot of peaks. Taking the 4^{th} minute as an example, there are 6 power peaks before reconfiguration. After optimization, power peaks have, respectively, decreased to 3 and 2 by the Sudoku method and GA. ASO has reduced the number of power peaks to one, which completely clears the local peaks. Hence, ASO has achieved a remarkable reconfiguration effect compared to other methods in this paper.

A timely provided PV array reconfiguration scheme is a significant evaluation criterion of the PV reconfiguration approach [39]. Table 4 provides the simulation time (s) of different reconfiguration methods compared with TCT configuration including ASO and other algorithms. The provided time data are calculated by each algorithm's averaged running time in the presented three cases. To ensure the fairness of each algorithm's simulation time, the population size and the max iteration number are all set to be 25 and 200, respectively. The provided data have shown that the operating speed of ASO is the highest, while GA ranks second. So it is obvious that the proposed approach is preferable to the other algorithms used in this paper.

4.2. Hardware-in-the-Loop Experiment. To ensure the real-time response capability of the used PV array, this paper proposed real-time hardware-in-the-loop experiment based

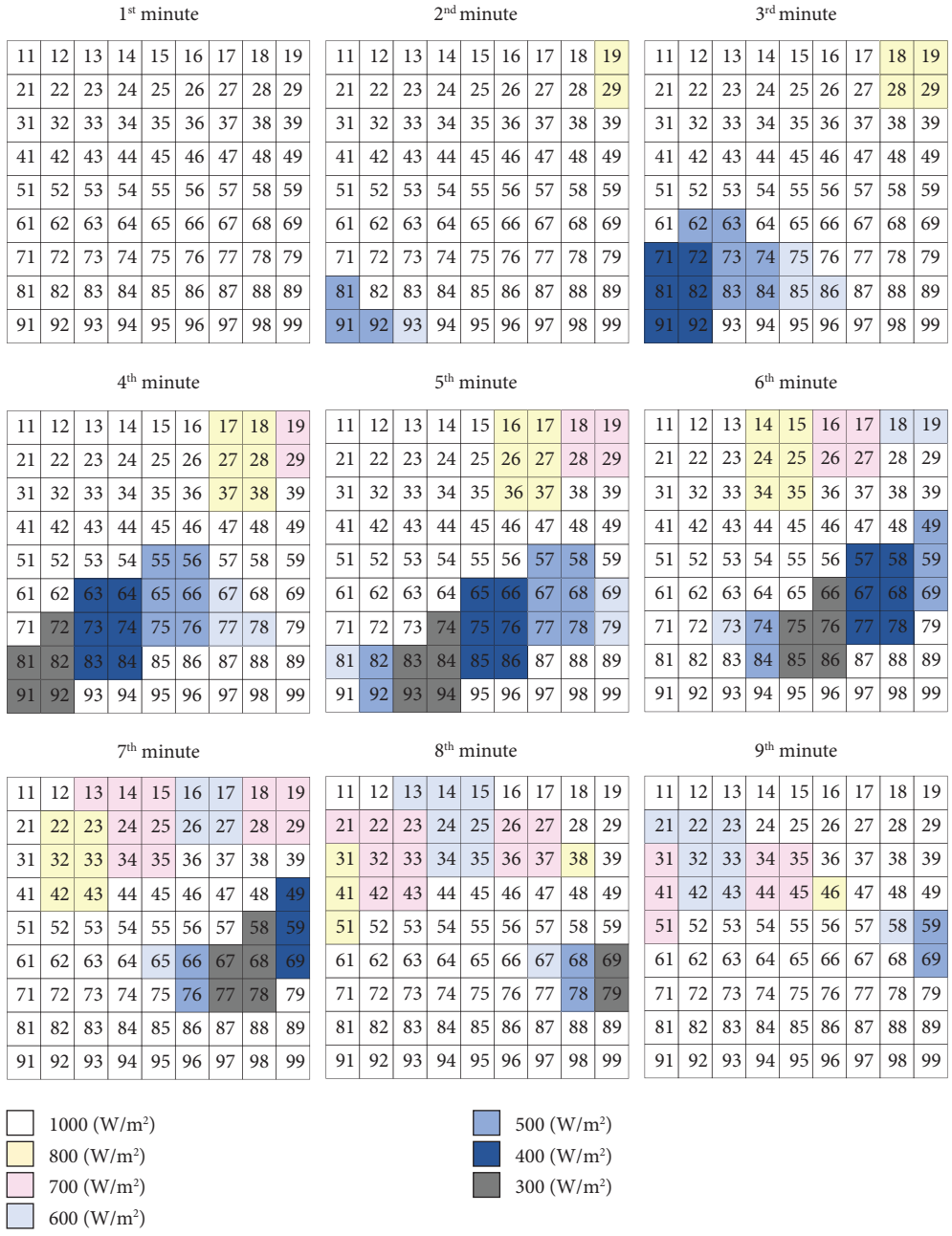

Figure 5: The irradiation of each PV array in 9 minutes under the shadow of moving clouds.

on the RTLAB platform to evaluate the output characteristics under different temperatures and irradiance which is shown in Figure 8. For comparison, a simulation based on the MATLAB 2020a platform is introduced. Figures 9 and 10, respectively, show that the simulation results under different temperatures and irradiation obtained by the RTLAB platform and MATLAB platforms basically coincide. These results illustrated that the maximum output power of the PV array is linearly rated to input irradiation. By contrast, the input temperature has little influence on the maximum output power. Because the above two platforms remain consistent through the simulation, all the case

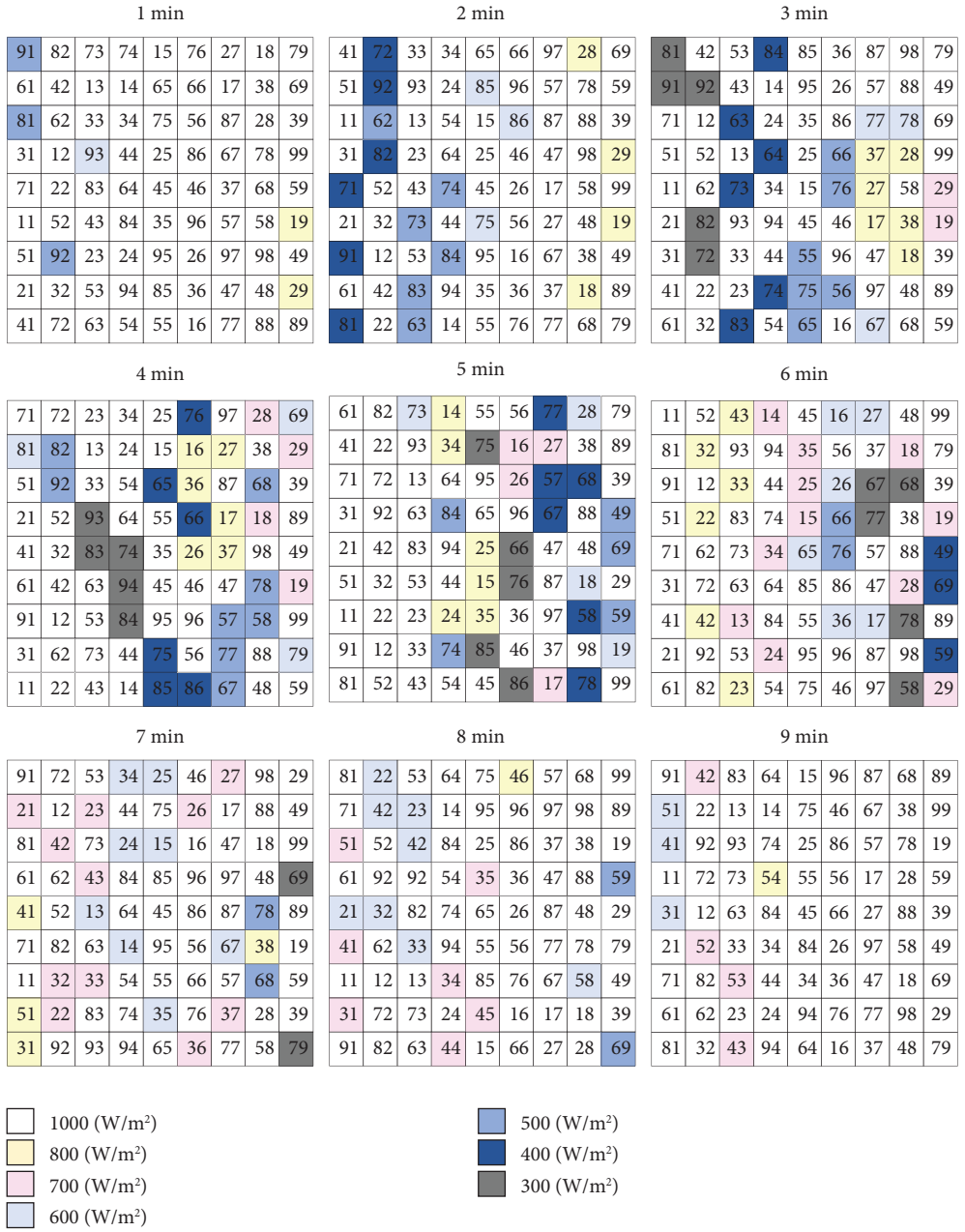

Figure 6: Optimal irradiation scheme of PV arrays by ASO in 9 minutes under the shadow of moving clouds.

Table 3: Comparison of the simulation results of each algorithm.

Time	Before optimization	Sudoku	ACO			GA			PSO			ASO		
	P_{out} (kW)	P_{out} (kW)	P_{max} (kW)	P_{min} (kW)	STD (W)	P_{max} (kW)	P_{min} (kW)	STD (W)	P_{max} (kW)	P_{min} (kW)	STD (W)	P_{max} (kW)	P_{min} (kW)	STD (W)
1 min	19.163	20.928	21.432	21.432	0	21.432	21.181	103.48	21.432	21.432	0	21.432	21.432	0
2 min	15.297	18.407	19.92	19.415	171.6	19.668	18.659	246.78	19.92	19.163	202.05	19.92	19.668	56.38
3 min	14.344	15.913	18.407	17.903	152.5	18.407	16.642	312.59	18.407	17.903	173.06	18.659	18.155	123.39
4 min	13.868	16.894	17.903	17.65	123.39	17.903	16.642	332.05	18.155	17.398	238.16	18.155	17.65	184.75
5 min	14.793	16.642	18.407	18.155	126.74	18.155	17.146	286.62	18.659	17.903	249.15	18.659	18.155	150.85
6 min	15.381	17.146	18.659	18.155	128.7	18.407	16.894	387.83	18.659	18.155	152.5	18.659	18.407	126.74
7 min	16.642	18.659	19.415	19.163	112.02	19.415	18.155	281.91	19.668	19.163	214.89	19.668	19.163	161.56
8 min	17.903	19.668	20.424	20.172	103.48	20.424	19.668	222.54	20.676	20.172	180.63	20.676	20.172	115.69
9 min	19.668	20.172	21.685	21.685	0	21.685	21.181	208.17	21.685	21.685	0	21.685	21.685	0
Mismatch loss (kW) (total)	79.875	62.505	50.682	53.204	—	51.348	60.766	—	49.673	53.960	—	49.421	52.447	—
Fill factor (average)	0.5634	0.6299	0.6752	0.6655	—	0.6723	0.6366	—	0.6791	0.6626	—	0.6800	0.6684	—

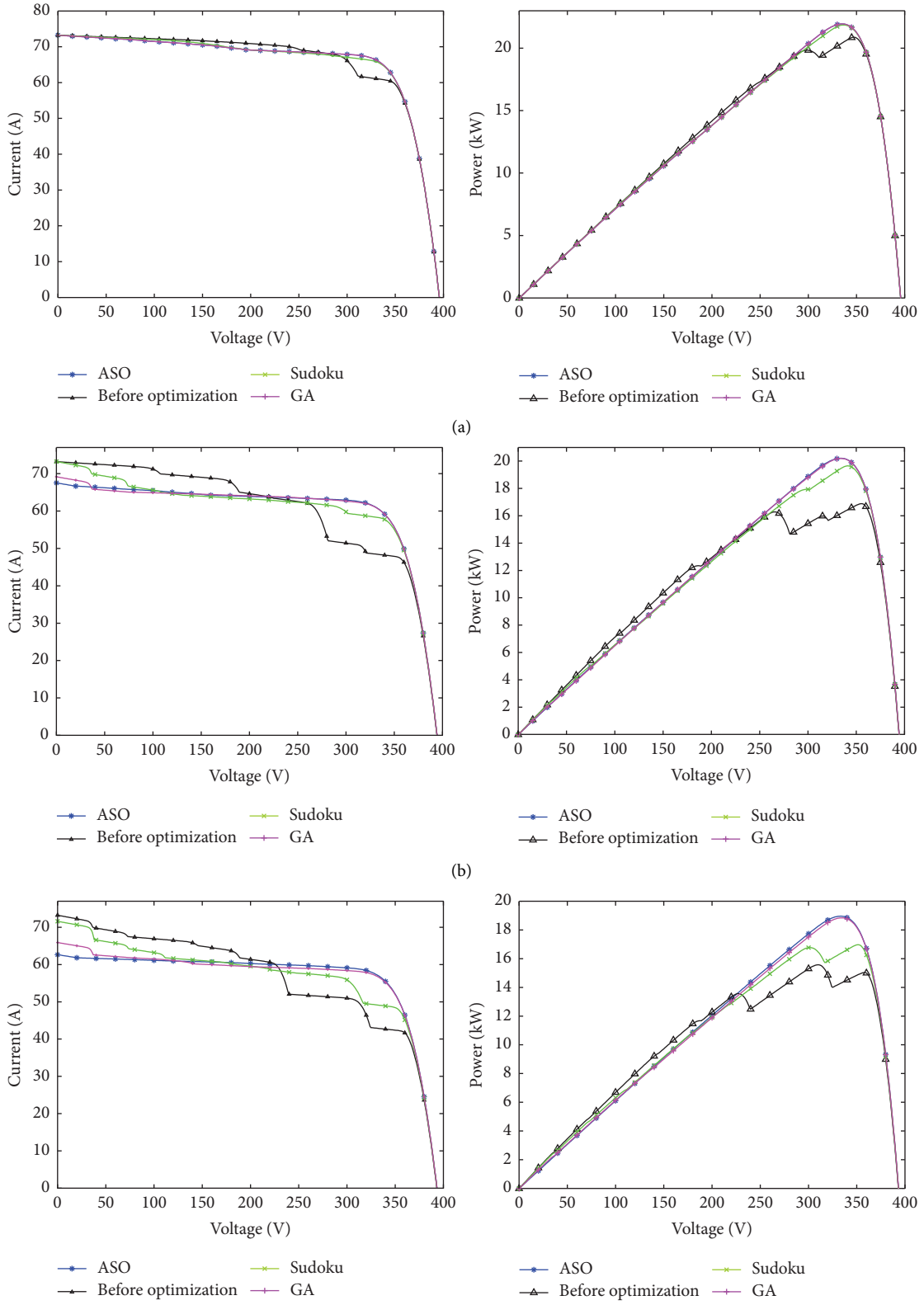

Figure 7: Continued.

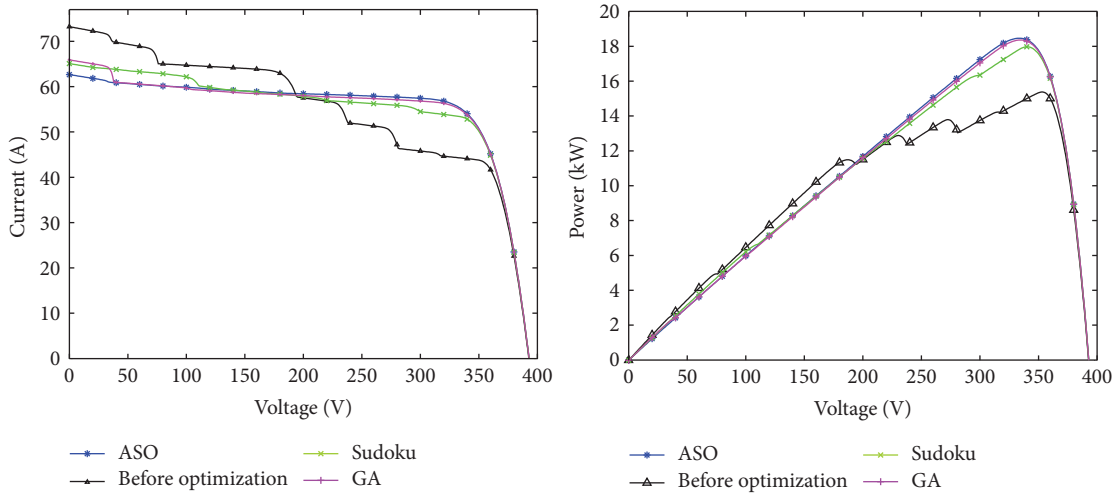

(d)

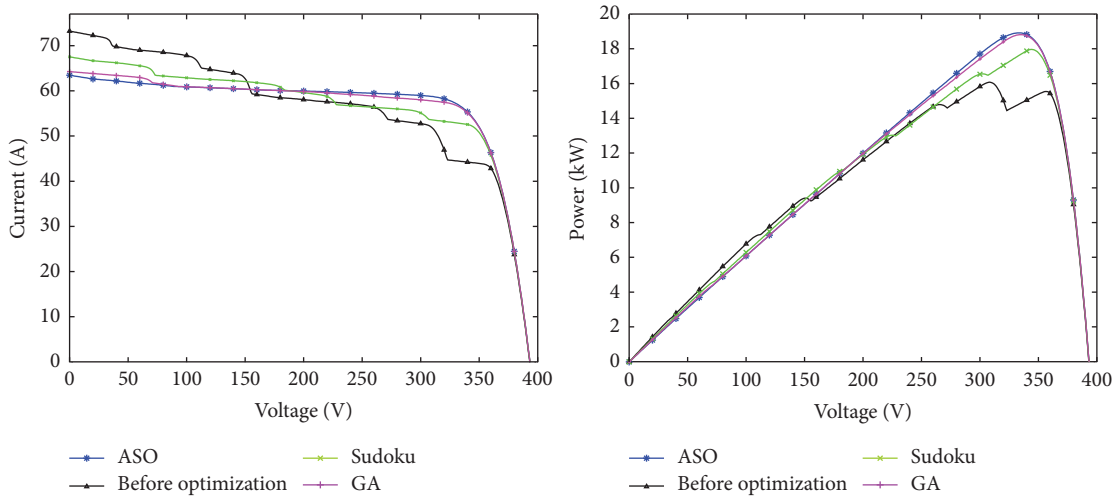

(e)

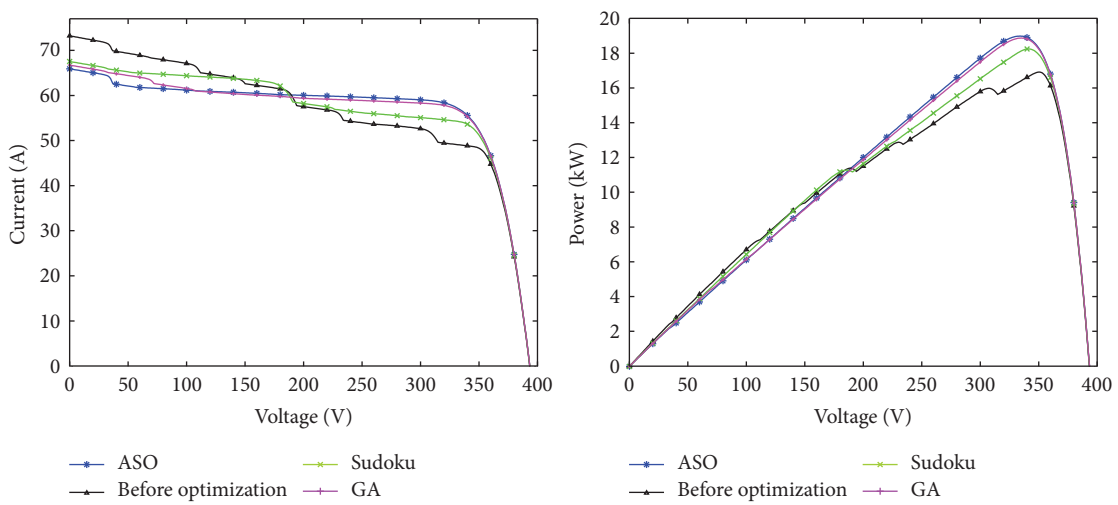

(f)

Figure 7: Continued.

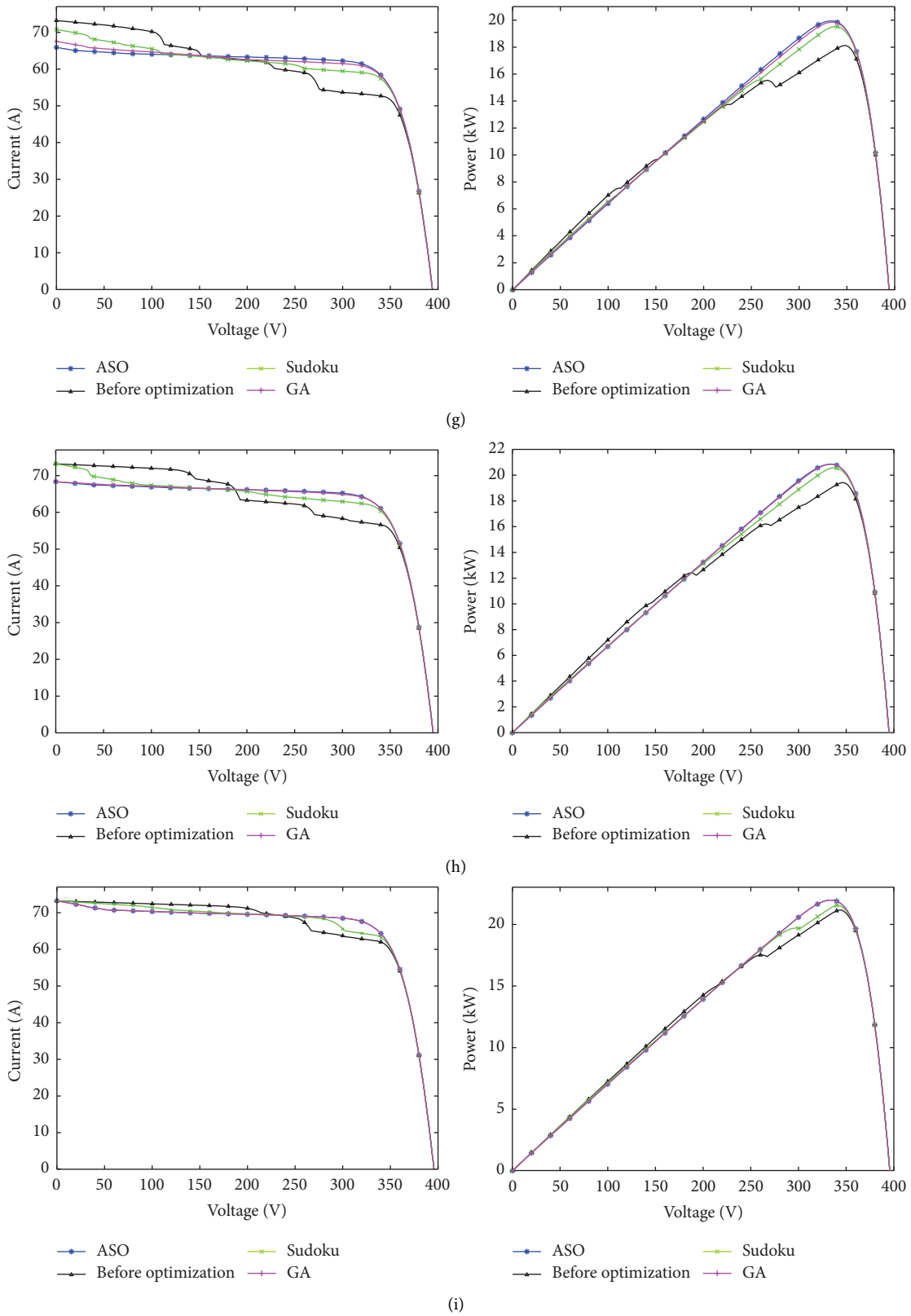

FIGURE 7: *I-U* and *P-U* curves of PV arrays with the PSC of moving clouds in 9 minutes: (a) 1 min; (b) 2 min; (c) 3 min; (d) 4 min; (e) 5 min; (f) 6 min; (g) 7 min; (h) 8 min; (i) 9 min.

Table 4: The simulation time (s) of different reconfiguration methods.

Time (s)	1 min	2 min	3 min	4 min	5 min	6 min	7 min	8 min	9 min	Average
ASO	0.456	0.513	0.529	0.507	0.504	0.48	0.528	0.511	0.514	0.505
ACO	5.408	5.438	5.385	5.448	5.407	5.47	5.386	5.404	5.389	5.47
GA	1.151	1.478	1.151	1.28	1.121	1.318	1.358	1.499	1.274	1.277
PSO	4.798	4.724	4.717	4.698	4.633	4.593	4.567	4.567	4.603	4.649

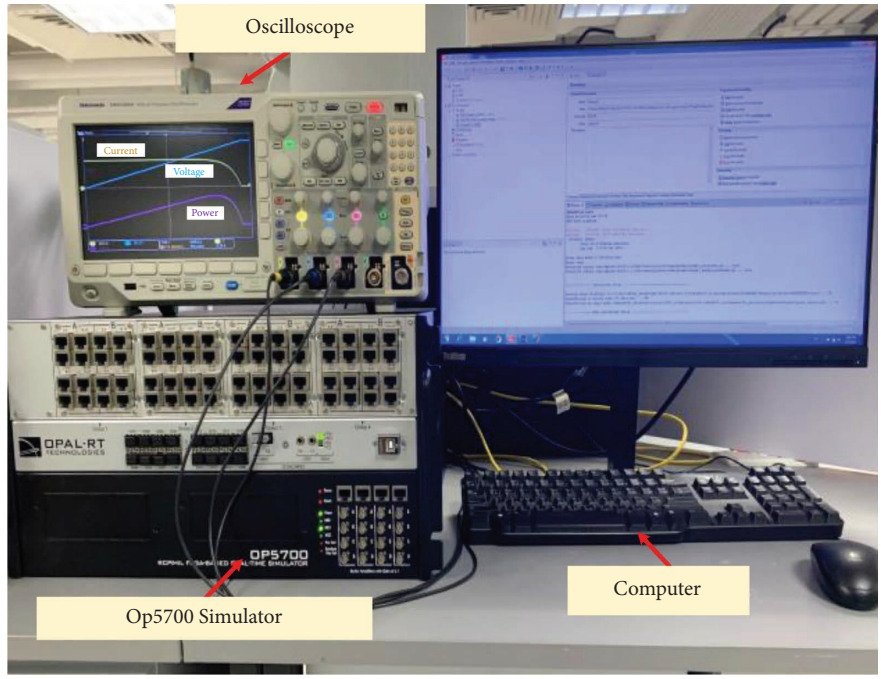

Figure 8: The RTLAB platform-based real-time hardware-in-the-loop experiment.

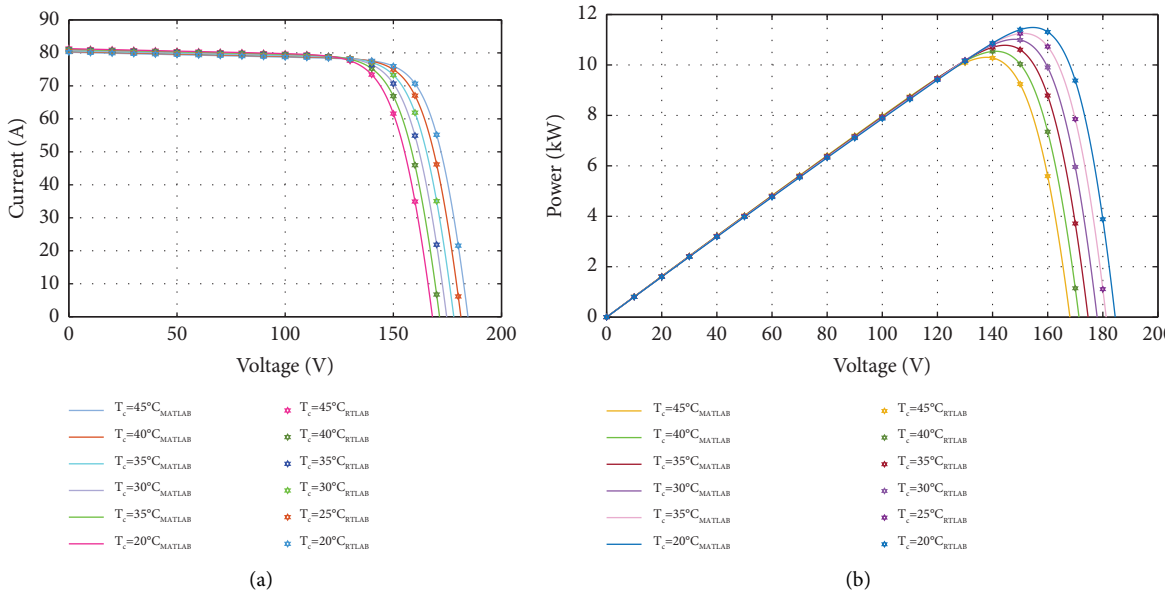

Figure 9: Output characteristic of each PV array obtained by RTLAB and MATLAB platforms under different temperatures when $G = 1000\ \mathrm{W/m^2}$: (a) *I-U* curves and (b) *P-U* curves.

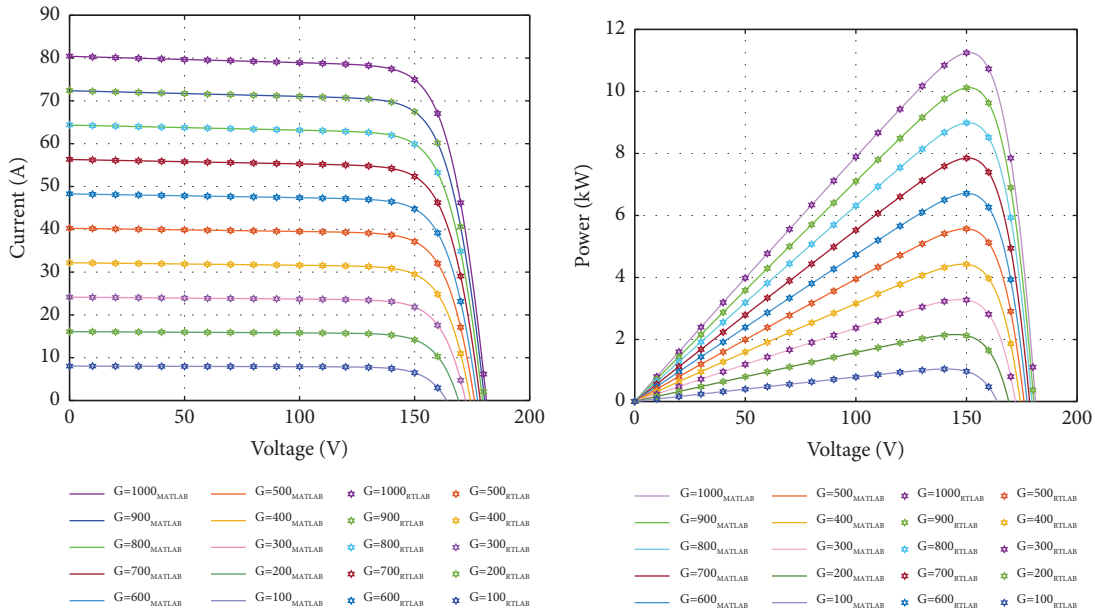

FIGURE 10: Output characteristic of each PV array obtained by RTLAB and MATLAB platforms under different irradiations when $T = 25^{\circ}C$: (a) *I-U* curves and (b) *P-U* curves.

studies in this paper are undertaken in MATLAB R2020a by using a desktop computer with Intel(R) Core TM i7-8650U CPU at 2.11 GHz with 8 GB of RAM.

5. Conclusions

This paper proposed an ASO-based PV array reconfiguration technique. This approach is realized by discretizing the original ASO algorithm and combining it with a PV reconfiguration approach. ASO can provide the optimal solution in real time; thus, the local optimal solution can be avoided. By comparing the output power, mismatch loss, fill factor, standard deviation, and output characteristic curves of ASO, Sudoku, ACO, GA, and PSO quantitatively, the superiority of ASO is proved. Moreover, the HIL experiment has proved the hardware feasibility of the ASO-based PV reconfiguration method. Besides, a novel shading mode of moving clouds is proposed, which can be applied in related studies for researchers. Future research will address the practical problems of ASO, the defects of ASO should be improved to improve the efficiency of algorithm optimization, and ASO should be applied to larger photovoltaic arrays [40].

Data Availability

The constraint and parameter data used to support the findings of this study are included within the article.

Conflicts of Interest

The authors declare that they have no conflicts of interest.

Authors' Contributions

Dahu Li was responsible for conceptualization and writing and editing the manuscript. Hongyu Zhou was responsible for writing the original draft and investigation. Yue Zhou was responsible for reviewing the manuscript and supervision. Yuzhe Rao was responsible for conceptualization and resources. Wei Yao was responsible for writing and reviewing the manuscript and supervision.

Acknowledgments

This work was jointly supported by the Science and Technology Project of State Grid Hubei Electric Power Co., Ltd. (Research on Key Technologies of Operation and Control of Hubei New Power System for Multi UHVDC Feed in and New Energy Base Development, No. 52150521000W).

References

[1] Z. T. Shi, W. Yao, Z. P. Li et al., "Artificial intelligence techniques for stability analysis and control in smart grids: methodologies, applications, challenges and future directions," *Applied Energy*, vol. 278, Article ID 115733, 2020.

[2] H. Y. Zhou, W. Yao, K. Y. Sun, X. M. Ai, J. Y. Wen, and S. J. Cheng, "Characteristic investigation and overvoltage suppression of MMC-HVDC integrated offshore wind farms under onshore valve-side SPG fault," *IEEE Transactions on Power Systems*, 2023.

[3] X. Q. Fu, Q. Guo, and H. Sun, "Statistical machine learning model for stochastic optimal planning of distribution networks considering a dynamic correlation and dimension

reduction," *IEEE Transactions on Smart Grid*, vol. 11, no. 4, pp. 2904–2917, 2020.

[4] B. Yang, B. Q. Liu, H. Y. Zhou et al., "A critical survey of technologies of large offshore wind farm integration: summary, advances, and perspectives," *Protection and Control of Modern Power Systems*, vol. 7, no. 1, p. 17, 2022.

[5] X. T. Peng, W. Yao, C. Yan, J. Y. Wen, and S. J. Cheng, "Two-stage variable proportion coefficient based frequency support of grid-connected DFIG-WTs," *IEEE Transactions on Power Systems*, vol. 35, no. 2, pp. 962–974, 2020.

[6] H. Y. Zhou, W. Yao, K. Y. Sun, Y. F. Zhao, X. M. Ai, and J. Y. Wen, "A multi-level coordinated DC overcurrent suppression scheme for symmetrical bipolar MMC-HVDC integrated offshore wind farms," *International Journal of Electrical Power & Energy Systems*, vol. 147, Article ID 108880, 2023.

[7] H. Y. Zhou, W. Yao, X. M. Ai, J. Zhang, J. Y. Wen, and C. H. Li, "Coordinated power control of electrochemical energy storage for mitigating subsequent commutation failures of HVDC," *International Journal of Electrical Power & Energy Systems*, vol. 134, 2022.

[8] H. Y. Zhou, W. Yao, M. Zhou, X. M. Ai, J. Y. Wen, and S. J. Cheng, "Active energy control for enhancing AC fault ride-through capability of MMC-HVDC connected with offshore wind farms," *IEEE Transactions on Power Systems*, p. 1, 2022.

[9] X. Q. Fu, "Statistical machine learning model for capacitor planning considering uncertainties in photovoltaic power," *Protection and Control of Modern Power Systems*, vol. 7, pp. 5–63, 2022.

[10] X. Q. Fu and H. Niu, "Key technologies and applications of agricultural energy internet for agricultural planting and fisheries industry," *Information Processing in Agriculture*, 2022.

[11] S. Soulayman, M. Hamoud, M.-A. Hababa, and W. Sabbagh, "Feasibility of solar tracking system for PV panel in sunbelt region," *Journal of Modern Power Systems and Clean Energy*, vol. 9, no. 2, pp. 395–403, 2021.

[12] H. Patel and V. Agarwal, "MATLAB-based modeling to study the effects of partial shading on PV array characteristics," *IEEE Transactions on Energy Conversion*, vol. 23, no. 1, pp. 302–310, 2008.

[13] N. Belhaouas, M. S. A. Cheikh, P. Agathoklis et al., "PV array power output maximization under partial shading using new shifted PV array arrangements," *Applied Energy*, vol. 187, pp. 326–337, 2017.

[14] V. V. Kuvshinov, L. M. Abd Ali, E. G. Kakushina, B. L. Krit, N. V. Morozova, and V. V. Kuvshinova, "Studies of the PV array characteristics with changing array surface irradiance," *Applied Solar Energy*, vol. 55, no. 4, pp. 223–228, 2019.

[15] R. Ahmad, A. F. Murtaza, H. Ahmed Sher, U. Tabrez Shami, and S. Olalekan, "An analytical approach to study partial shading effects on PV array supported by literature," *Renewable and Sustainable Energy Reviews*, vol. 74, pp. 721–732, 2017.

[16] A. Bidram, A. Davoudi, and R. S. Balog, "Control and circuit techniques to mitigate partial shading effects in photovoltaic arrays," *IEEE Journal of Photovoltaics*, vol. 2, no. 4, pp. 532–546, 2012.

[17] R. K. Pachauri, O. P. Mahela, A. Sharma et al., "Impact of partial shading on various PV array configurations and different modeling approaches: a comprehensive review," *IEEE Access*, vol. 8, pp. 181375–181403, 2020.

[18] I. Nasiruddin, S. Khatoon, M. F. Jalil, and R. Bansal, "Shade diffusion of partial shaded PV array by using odd-even structure," *Solar Energy*, vol. 181, pp. 519–529, 2019.

[19] F. Belhachat and C. Larbes, "PV array reconfiguration techniques for maximum power optimization under partial shading conditions: a review," *Solar Energy*, vol. 230, pp. 558–582, 2021.

[20] B. Yang, R. Shao, M. Zhang et al., "Socio-inspired democratic political algorithm for optimal PV array reconfiguration to mitigate partial shading," *Sustainable Energy Technologies and Assessments*, vol. 48, Article ID 101627, 2021.

[21] R. Bakhshi and J. Sadeh, "A comprehensive economic analysis method for selecting the PV array structure in grid–connected photovoltaic systems," *Renewable Energy*, vol. 94, pp. 524–536, 2016.

[22] B. I. Rani, G. S. Ilango, and C. Nagamani, "Enhanced power generation from PV array under partial shading conditions by shade dispersion using Su Do Ku configuration," *IEEE Transactions on Sustainable Energy*, vol. 4, no. 3, pp. 594–601, 2013.

[23] S. Vijayalekshmy, G. R. Bindu, and S. R. Iyer, "Performance comparison of Zig-Zag and Su Do Ku schemes in a partially shaded photovoltaic array under static shadow conditions," in *Proceedings of the 2017 Innovations in Power and Advanced Computing Technologies*, pp. 1–6, Vellore, India, April 2017.

[24] M. S. S. Nihanth, J. P. Ram, D. S. Pillai, A. M. Ghias, A. Garg, and N. Rajasekar, "Enhanced power production in PV arrays using a new skyscraper puzzle based one-time reconfiguration procedure under partial shade conditions (PSCs)," *Solar Energy*, vol. 194, pp. 209–224, 2019.

[25] R. Venkateswari and N. Rajasekar, "Power enhancement of PV system via physical array reconfiguration based Lo Shu technique," *Energy Conversion and Management*, vol. 215, Article ID 112885, 2020.

[26] O. Bingöl and B. Özkaya, "Analysis and comparison of different PV array configurations under partial shading conditions," *Solar Energy*, vol. 160, pp. 336–343, 2018.

[27] D. Yousri, T. S. Babu, E. Beshr, M. B. Eteiba, and D. Allam, "A robust strategy based on marine predators algorithm for large scale photovoltaic array reconfiguration to mitigate the partial shading effect on the performance of PV system," *IEEE Access*, vol. 8, pp. 112407–112426, 2020.

[28] A. Tabanjat, M. Becherif, and D. Hissel, "Reconfiguration solution for shaded PV panels using switching control," *Renewable Energy*, vol. 82, pp. 4–13, 2015.

[29] A. M. Ajmal, T. Sudhakar Babu, V. K. Ramachandaramurthy, D. Yousri, and J. B. Ekanayake, "Static and dynamic reconfiguration approaches for mitigation of partial shading influence in photovoltaic arrays," *Sustainable Energy Technologies and Assessments*, vol. 40, Article ID 100738, 2020.

[30] G. Sai Krishna and T. Moger, "Reconfiguration strategies for reducing partial shading effects in photovoltaic arrays: State of the art," *Solar Energy*, vol. 182, pp. 429–452, 2019.

[31] R. N. Shao, B. Yang, and Y. Han, "Evaluations of practical engineering application of photovoltaic reconfiguration technology," *Frontiers in Energy Research*, vol. 9, Article ID 831249, 2022.

[32] F. H. Gandoman, F. Raeisi, and A. Ahmadi, "A literature review on estimating of PV-array hourly power under cloudy weather conditions," *Renewable and Sustainable Energy Reviews*, vol. 63, pp. 579–592, 2016.

[33] M. Jazayeri, K. Jazayeri, and S. Uysal, "Adaptive photovoltaic array reconfiguration based on real cloud patterns to mitigate

effects of non-uniform spatial irradiance profiles," *Solar Energy*, vol. 155, pp. 506–516, 2017.

[34] N. A. Rajan, K. D. Shrikant, B. Dhanalakshmi, and N. Rajasekar, "Solar PV array reconfiguration using the concept of Standard deviation and genetic algorithm," *Energy Procedia*, vol. 117, pp. 1062–1069, 2017.

[35] W. Zhao, L. Wang, and Z. Zhang, "Atom search optimization and its application to solve a hydrogeologic parameter estimation problem," *Knowledge-Based Systems*, vol. 163, pp. 283–304, 2019.

[36] S. Krishnan G, S. Kinattingal, S. P. Simon, and P. S. R. Nayak, "MPPT in PV systems using ant colony optimisation with dwindling population," *IET Renewable Power Generation*, vol. 14, no. 7, pp. 1105–1112, 2020.

[37] S. N. Deshkar, S. B. Dhale, J. S. Mukherjee, T. S. Babu, and N. Rajasekar, "Solar PV array reconfiguration under partial shading conditions for maximum power extraction using genetic algorithm," *Renewable and Sustainable Energy Reviews*, vol. 43, pp. 102–110, 2015.

[38] T. S. Babu, J. P. Ram, T. Dragičević, M. Miyatake, F. Blaabjerg, and N. Rajasekar, "Particle swarm optimization based solar PV array reconfiguration of the maximum power extraction under partial shading conditions," *IEEE Transactions on Sustainable Energy*, vol. 9, no. 1, pp. 74–85, 2018.

[39] T. S. Babu, D. Yousri, and K. Balasubramanian, "Photovoltaic array reconfiguration system for maximizing the harvested power using population-based algorithms," *IEEE Access*, vol. 8, pp. 109608–109624, 2020.

[40] B. Yang, H. Ye, J. Wang et al., "PV arrays reconfiguration for partial shading mitigation: recent advances, challenges and perspectives," *Energy Conversion and Management*, vol. 247, Article ID 114738, 2021.